

## Electronic states of doped semiconductor superlattices in magnetic and electric fields

Sergio E. Ulloa

*Department of Physics and Astronomy and Condensed Matter and Surface Sciences Program, Ohio University,  
Athens, Ohio 45701-2979*

George Kirczenow

*Physics Department, Simon Fraser University, Burnaby, British Columbia, Canada V5A 1S6*

(Received 16 October 1987)

A theoretical treatment of the effects of external fields on the electronic properties of doped semiconductor superlattices is presented. Self-consistent calculations of the level structure in the presence of strong magnetic fields reveal the existence of surfacelike states associated with the depletion regions at the ends of the superlattice. These states lie in the gap between Landau levels during Landau-level emptying and closely track the Fermi energy throughout the range of magnetic fields where the Hall plateaus occur. These results explain important features observed in recent experiments by Störmer *et al.*, such as the Hall quantization index and the anomalously small activation energy. The character of the surfacelike states can be strongly affected by varying the applied magnetic field and especially by the simultaneous application of an electric field in the direction perpendicular to the layers. The large sensitivity to applied fields suggests novel experimental arrangements which would directly probe the density of states of the system.

### I. INTRODUCTION

Research on multilayer semiconductor structures has attracted increasing attention over the past few years.<sup>1,2</sup> Much of this work has been stimulated by the possibility of being able to carefully control the electronic properties of synthesized materials over quite a wide range of physical parameters. This most important feature has been used to study a variety of very interesting physical phenomena as well as to explore novel device applications. Detailed understanding of the electronic properties of these systems is rapidly increasing and further advances are needed to fully exploit all their possibilities.

In this paper we present a description of the energy-level structure and corresponding charge distribution across a realistic semiconductor superlattice in the presence of strong magnetic fields and gate voltages. We show that the level structure exhibits a very complex behavior as a function of the applied fields which includes the creation of surfacelike states associated with the depletion regions near the ends of the structure. An interesting prediction of our theory is the possibility of changing the surfacelike trait of these states to a more bulklike character by changing the magnetic field and/or the electric field applied to the system. This provides a unique set of conditions by which to study a type of transition in which the confinement in one direction can be easily varied. We discuss the role of these states in certain experiments, especially the features of recent quantum-Hall-effect observations by Störmer *et al.*<sup>3</sup> Indeed, the analysis of the level structure provides a detailed explanation of the Hall quantization index and especially of the puzzling small activation energy measured for the highest Hall plateau. We also propose that the additional application of a potential difference across the superlattice chain in a Hall configuration would pro-

vide an interesting alternative probe of the density of states within the Landau bands, a question of great current interest.<sup>4-6</sup>

In this work we will focus our attention on the so-called type-I semiconductor superlattices. This choice was motivated by the experimental system of Ref. 3 but our model can be easily generalized to other types of tunneling superlattices. These structures are fabricated from layers of a material such as GaAs alternating with layers of the alloy  $\text{Al}_x\text{Ga}_{1-x}\text{As}$ . Since the latter material has a larger energy gap than GaAs, and the band discontinuities align appropriately, the free electrons or holes available in the system (from either photoexcitation or ionized impurities) will be confined mostly to the GaAs layers. The heterostructures can also be doped during growth with well-controlled profiles (modulation doping),<sup>1,2,7</sup> which provides for further versatility since it is then possible to spatially separate the charge carriers from the ionized impurities (if the latter are placed in the  $\text{Al}_x\text{Ga}_{1-x}\text{As}$  layers), greatly increasing the carrier mobility. The term superlattice is usually reserved in the literature for those heterostructure systems with thin constituent layers, which allow for carrier tunneling in the direction perpendicular to the growth direction. In this type of system the carriers will have a three-dimensional, albeit anisotropic, dispersion relation, unlike the so-called multiple-quantum-well structures which one can identify with a stack of two-dimensional systems.

The typical growth process of semiconductor superlattices is usually associated with defect states near the end layers of the structure. These states are related either to deep impurities in the substrate materials commonly used, or to surface states generated by the termination of the layer growth.<sup>3,8</sup> These midgap levels at the ends of a superlattice have been reported in the literature for quite some time; however, a more systematic study of their

properties has not appeared, while other interface levels are being actively studied.<sup>9</sup> Since the defect levels generally lie deep in the energy gap of the semiconductor structure they provide a reservoir of electronic traps which pins the Fermi level of the system. This pinning affects the electronic level structure of doped superlattices by producing depletion regions at the layers near the top and bottom of the structure.<sup>3,8</sup> A semiclassical treatment is helpful in giving the extent of the depletion region and associated electrostatic potential but does not address the quantum-mechanical nature of the resulting electronic states. A detailed understanding of this depletion-layer effect is of considerable interest since it could affect the various physical processes for which the superlattices are grown in the first place.

Here we present the results of self-consistent calculations of the energy-level structure of these superlattices and the associated charge profiles across the structure in the presence of an applied magnetic field and a gatelike voltage. The remainder of this work is organized as follows.<sup>10</sup> Section II describes the model used in the calculation of the level structure. In Sec. III we present results of the self-consistent calculations of the energy levels and discuss the character of the associated wave functions as a function of the magnetic field applied. We also discuss the application of a simultaneous gatelike voltage across the superlattice chain and its effect on the electronic levels. Finally, Sec. IV presents the consequences of the resulting level structure for the quantum Hall experiment and we discuss other experimental arrangements where these levels would produce important observable effects.

## II. MODEL

A type-I semiconductor superlattice, as described in the Introduction, may be viewed as a set of potential wells and barriers for electrons (or holes) along the direction perpendicular to the layers ( $z$ -axis direction). The defining features of this type of Kronig-Penney model system are given by a fraction of the difference in energy gap between the two materials at the  $\Gamma$  point (fraction believed to be about 65%, of a difference which in turn depends on the alloy composition  $x$  in the case of GaAs/Al <sub>$x$</sub> Ga <sub>$1-x$</sub> As),<sup>1,11</sup> as well as the corresponding layer thicknesses. This representation of the semiconductor superlattice is in reasonably good agreement with the observed main characteristics of these systems.<sup>2</sup> However, a calculation of the electronic level structure in the case of a doped superlattice containing free carriers should consider the existence of midgap states at both ends of the system. Because of the necessary self-consistency between the potential and charge distribution in the system, the midgap states strongly affect the resulting electronic states. This gives rise to depletion regions near the ends of the superlattice and associated electronic states, which are not described by the simple periodic-potential model.

In this calculation we make use of a basis of Wannier states belonging to the lowest electron miniband to describe electron propagation in the  $z$  direction.<sup>12</sup> These Wannier states  $\phi_j(z)$  are centered on the different poten-

tial wells (GaAs layers), where  $j$  is the layer index (equal to 1 to  $N$ ). Correspondingly, the Hamiltonian which describes the motion along the  $z$  direction is given by

$$H_z = \sum_{j,\sigma} (v_j c_{j,\sigma}^\dagger c_{j,\sigma} - t c_{j+1,\sigma}^\dagger c_{j,\sigma} - t c_{j,\sigma}^\dagger c_{j+1,\sigma}), \quad (1)$$

where  $c_{j,\sigma}^\dagger$  is the creation operator associated with the state  $\phi_j$  and spin  $\sigma$ , and  $t$  is the nearest-neighbor hopping matrix element. The value of  $t$  is determined from the bandwidth  $W$  of a periodic system by  $t = W/4$ , as in any one-dimensional tight-binding model.<sup>13</sup> The diagonal terms in Eq. (1) represent the self-consistent potential felt by the electrons. This potential  $v(z)$  contains both the electron-electron interaction and the electron-ion background interaction, and obeys Poisson's equation which in discretized form is given by

$$v_{j+1} - 2v_j + v_{j-1} = 4\pi e^2 a (\rho_+ - \rho_j) / \epsilon, \quad (2)$$

where  $\rho_+$  is the positive background density,  $\rho_j$  is the electronic surface density of layer  $j$ ,  $a$  is the superlattice period, and  $\epsilon$  is the average semiconductor dielectric constant. Notice that the solution to this finite-difference equation is subject to complementary boundary conditions, just as the differential equation it approximates. The appropriate boundary conditions to this problem should incorporate the existence of the midgap states mentioned above. In order to model the situation in a real superlattice system, the potential values at the ends of the structure are kept fixed with respect to the Fermi energy  $\mu$  of the system. At one end of the superlattice we set

$$v_{N+1} = \mu + \delta, \quad (3a)$$

where the constant value of  $\delta$  chosen produces a pinning of the Fermi level at approximately 0.8 eV below the edge of the conduction band of GaAs (i.e.,  $v_N - \mu \approx 0.8$  eV), corresponding to the binding energy of the deep levels.

The other end is assumed to be attached to an impurity-free buffer region of thickness  $L$  (as is the case in the experimental system of Ref. 3). The undoped GaAs buffer region is followed by a doped substrate which also provides midgap states at this end of the structure. The potential  $v(z)$  in the buffer region, since it is free of charges, has a linear dependence in position, with a uniform field given by  $-dv/dz = (v_0 - v_1)/a$ . The potential at the far end of the buffer is fixed at  $v(-L) = \mu + \delta'$ , with  $\delta'$  constant. From these two expressions and from  $v(0) = v_1$ , we find  $v(-L) = v_1 + (v_0 - v_1)L/a$ , or correspondingly,

$$v_0 = v_1 + (v_{N+1} - v_1 + \delta' - \delta)a/L, \quad (3b)$$

as the second boundary condition imposed on the solution of Eq. (2).

The second term on the right-hand side of Eq. (2) represents the electronic density, and its dependence on the specific eigenfunctions of the system will force a self-consistent solution of Eq. (2) and the diagonalization of the Hamiltonian of the system (of which  $H_z$  is the part describing the motion in the  $z$  direction), together with the boundary conditions provided by Eqs. (3). In the case

of a magnetic field along the  $z$  axis,  $\mathbf{B}=\hat{z}B$ , the in-plane motion Hamiltonian yields the well-known Landau-level structure,<sup>14</sup> whose eigenvalues are given in terms of the quantum numbers  $n$  ( $n=0,1,2,\dots$ ) and the spin  $z$  projection  $\sigma=\pm\frac{1}{2}$ , by

$$E_{n\sigma}=(n+\frac{1}{2})\hbar\omega_c+g\mu_B B\sigma, \quad (4)$$

where  $\omega_c=eB/m$  is the cyclotron frequency,  $m$  is the effective mass,  $\mu_B$  is the Bohr magneton, and  $g$  is the Landé factor appropriate to the system.<sup>15</sup> In this case, the electronic density per layer appearing in Eq. (2) can be written as

$$\rho_j=(2\pi a_c^2)^{-1}\sum_{m,n,\sigma}\int dE|b_j^m|^2g(E-E_{mn\sigma}), \quad (5)$$

where  $(2\pi a_c^2)^{-1}$  is the Landau-level degeneracy per unit area, and  $a_c=(\hbar/eB)^{1/2}$  is the magnetic length. The coefficients  $b_j^m$  describe the  $z$ -axis-motion eigenvector of  $H_z$  with eigenvalue  $E_m$ ,  $H_z\Phi_m=E_m\Phi_m$ , i.e.,

$$\Phi_m(z)=\sum_j b_j^m\phi_j(z). \quad (6)$$

The Gaussian function  $g(x)$  takes into account the impurity broadening of the levels,

$$g(x)=(2\pi\Gamma^2)^{-1/2}\exp(-x^2/2\Gamma^2), \quad (7)$$

with a large rms width  $\Gamma$ , which allows us to neglect the small thermal broadening present in experiments (i.e.,  $\Gamma\gg kT$ ). Indeed, simple estimates of  $\Gamma$  based on the electronic mobility  $\mu_0$  measured in these systems give  $\Gamma=e\hbar/2m\mu_0\approx 1$  meV.<sup>3,16</sup> The form chosen for the broadening function allows one to perform the integration in Eq. (5) analytically, reducing the expression for the areal electronic density at layer  $j$  to

$$\rho_j=(2\pi a_c^2)^{-1}\sum_{m,n,\sigma}|b_j^m|^2I_{mn\sigma}, \quad (8)$$

where  $I_{mn\sigma}=\{1-\text{erf}[(E_m+E_{n\sigma}-\mu)/\Gamma\sqrt{2}]\}/2$ , and  $\text{erf}(x)$  is the usual error function.

Equations (1), (2), and (8) together with the boundary conditions (3) form the set to be solved self-consistently for given values of the parameters characterizing the system. The specific chosen values model the system used in the experiments of Ref. 3, but they can clearly be changed according to the particular system of interest. Section III presents typical level structures obtained by the solution of the above equations.<sup>17</sup>

We are also interested in the effect of a gate voltage applied across the superlattice in the  $z$  direction since this would readily affect the extent of the depletion regions caused by the pinning of the Fermi level. The application of this voltage produces a charge imbalance which is compensated by the charging of the structure, changing the total amount of free electronic charge in the system one way or another depending on the sign of the bias, in a fashion similar to a gate voltage in modulation-doped field-effect transistor (MODFET) structures.<sup>18,19</sup> As is shown in the following section, the gate voltage applied simultaneously with the magnetic field produces significant changes in the level structure. This effect may

furthermore be used in the direct determination of the electronic density of states, as will be discussed later. A report of a very interesting experiment of this kind has recently appeared.<sup>3(b)</sup> We simulate the applied gate voltage by varying the parameter  $\delta$  which defines the value of the potential energy at the edge of the semiconductor superlattice. In the calculations reported in Sec. III, the effective gate voltage is defined as  $V_G=\delta_0-\delta$ , where  $\delta_0=1.6$  eV is the value in the unbiased system.<sup>17</sup> This variation in the parameter  $\delta$  would simulate the case in which the voltage at that end ( $j=N$ ) is applied with respect to the middle layers of the superlattice.

We should stress that the boundary conditions given by Eqs. (3) are designed to allow the total electron density in the system to be determined self-consistently, according to the Fermi energy. Here we have allowed the electronic density to vary in a manner as to maintain a constant Fermi level, since the system is assumed to have electrical connections to an external charge reservoir and to be in equilibrium with it.<sup>17</sup> The charge would flow through the contacts attached to the electronic system and would regulate itself. This is of special importance in the case of a gated system, as will be shown below, since the voltages applied across the structure will effectively empty or fill the layers of the superlattice in order to achieve electrostatic equilibrium.

### III. LEVEL STRUCTURE

In this section we present examples of the electronic level structure of superlattices in the presence of applied magnetic fields and gate voltages. All of the calculations were made for a system consisting of 30 periods of GaAs/AlGaAs layers (i.e.,  $N=30$ ), in order to allow direct comparison with the experiment of Ref. 3.

#### A. In a magnetic field

Figures 1 and 2 show the energy levels of an unbiased system with parameters given in Ref. 17, for different ranges of the applied magnetic field  $B$ . The eigenvalues  $E_{mn\sigma}=E_{n\sigma}+E_m$  are plotted relative to the Fermi level  $\mu$ , and only the center of each broadened level is shown. Notice that each Landau level is actually a band of width  $W\approx 4t$ , due to the  $z$ -direction dispersion. Figure 1 shows the region of magnetic field in which the second Landau band ( $n=1$ ) is being emptied, and Fig. 2 shows the region for the emptying of the third band ( $n=2$ ). A very important feature of both of these diagrams is the appearance of split-off levels (denoted by SS in Fig. 1) that lie in the gap region between consecutive Landau bands. Notice also that these levels track the Fermi level closely over a wide range of magnetic field values, and therefore remain only partially filled. The eigenvectors corresponding to these split-off states are strongly peaked near one of the ends of the chain, and decay rapidly towards the interior of the superlattice, within about two GaAs layers (see below). This surface-localized character is not unlike that of evanescent states appearing at crystal surfaces.<sup>13</sup> However, the surfacelike states in this superlattice system are typically extended over a much larger region (at least

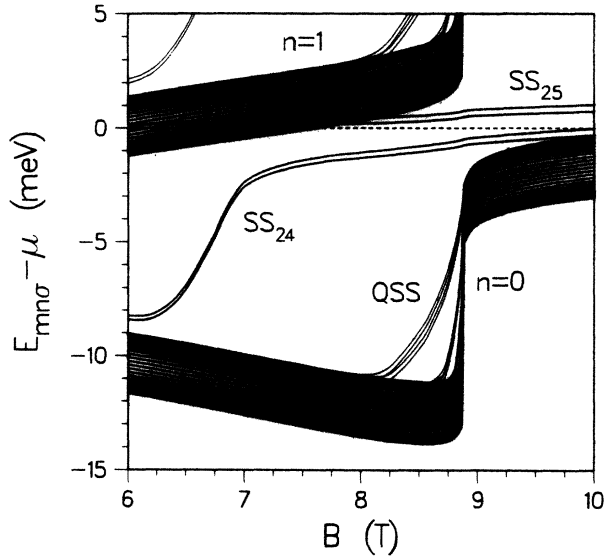


FIG. 1. Energy levels  $E_{mn\sigma}$  of a tunneling superlattice with respect to the Fermi energy  $\mu$  (dashed line) for lowest Landau indices  $n$ . Only center of each broadened level is shown ( $\Gamma=1$  meV).  $SS_m$  spin doublets correspond to the quantum numbers  $\sigma = \pm\frac{1}{2}$ ,  $n=0$ , and  $m=24$  (25) for levels below (above)  $\mu$ . QSS doublets correspond to  $\sigma = \pm\frac{1}{2}$ ,  $n=0$ , and  $m=22, 23$ .

a whole GaAs layer) and most importantly, *their surface-localized character is strongly affected by the variation of the applied magnetic field*, as can be seen in Fig. 3.

Figure 3 shows the  $z$ -motion eigenfunctions  $\Phi_m$  [i.e., the value of the  $b_j^m$  coefficients in Eq. (6)] associated with the two SS doublets shown in Fig. 1 (which correspond to the eigenvalues with quantum numbers  $n=0$ ,  $\sigma = \pm\frac{1}{2}$ ,

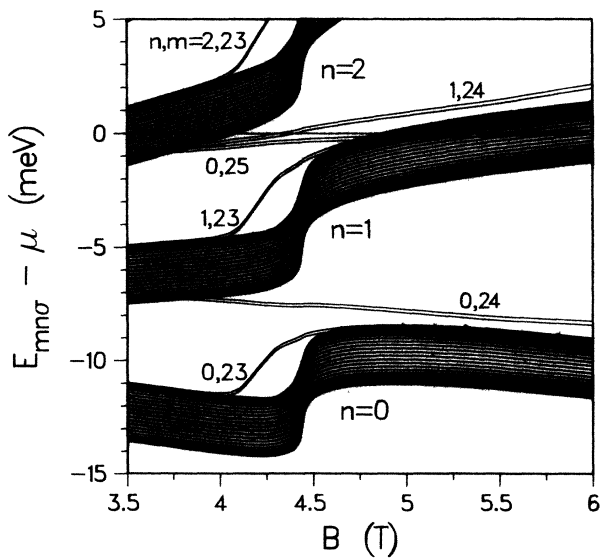


FIG. 2. Level structure at lower magnetic field. Here, the  $n=2$  band is being emptied. Notice SS states also present in the Landau gap regions. These spin doublets ( $\sigma = \pm\frac{1}{2}$ ) are labeled by their quantum numbers  $n, m$ .

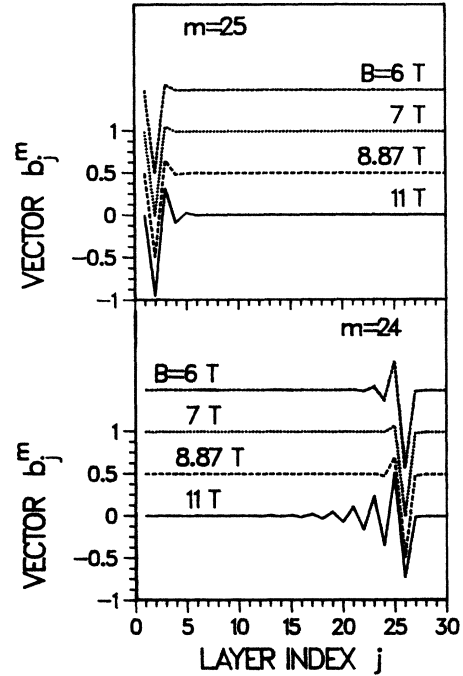


FIG. 3.  $z$ -motion eigenvectors of SS states in Fig. 1 for several values of magnetic field. Notice larger penetration for increasing field values, where eigenstates join band quasicontinuum, especially for  $m=24$  state. In each panel all traces but the lowest are successively displaced upwards by 0.5.

and  $m=24, 25$ ), for several values of the magnetic field. These states are mostly associated with a given end of the lattice ( $m=24$  with the right end,  $m=25$  with the left end), but their extension in the superlattice changes with the value of the magnetic field. Indeed, the eigenfunctions are strongly peaked at one given layer for fields  $B \lesssim 8.9$  T, corresponding to the larger splitting from the band, and become more “bulklike” as their eigenvalues approach the band, reducing their splitting. This is especially so in the case of the  $m=24$  doublet which joins the Landau band at about 10 T, while the doublet with  $m=25$  remains highly localized at the left end of the structure. Therefore, changing the magnetic field by about 2 T (from 8.9 to 11 T) increases the penetration (i.e., layers for which  $b_j^m \gg 0$ ) of the state  $\Phi_{24}$  by a factor of 3 and that of  $\Phi_{25}$  by only a factor of 2.

Figures 1 and 2 also show states (denoted by QSS) which have a tendency to peel off from the band quasicontinuum, but only for a small range of magnetic fields ( $\lesssim 1$  T), and indeed act as precursors of the total emptying of a Landau band. Moreover, the energy shifts of the QSS states are accompanied by an enhancement of their wave-function amplitude near the end layers, which makes them acquire a more surfacelike character. The  $z$ -motion eigenfunction  $\Phi_{23}$ , corresponding to one of the QSS states, is plotted in Fig. 4 for several values of magnetic field and shows clearly these effects. It is very interesting that the wave function associated with this state is much more sensitive to changes in magnetic field than that of the SS states even though the energy shifts are

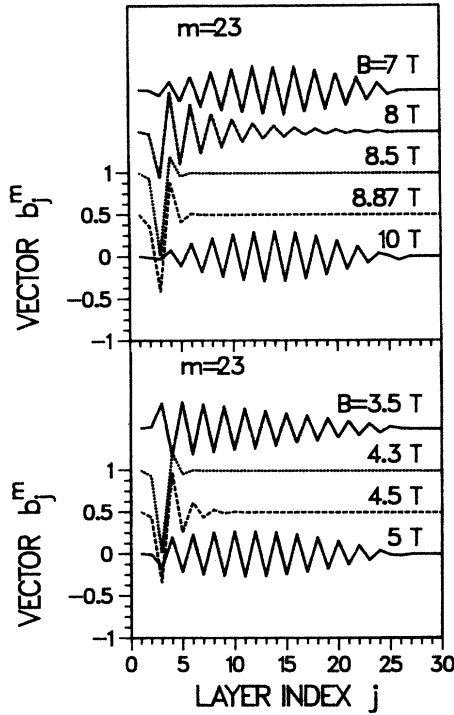


FIG. 4.  $z$ -motion eigenvector  $m = 23$  for two different ranges of  $B$ . Notice drastic changes in extension for this QSS state which peaks near the left end of the structure when its splitting from the Landau band is greatest (see Figs. 1 and 2).

smaller than those of  $\Phi_{24}$  and  $\Phi_{25}$ . This different behavior may be related to the complete occupation of the low-lying doublet, as opposed to only a partial filling of the others. Notice also that  $\Phi_{23}$  is greatly affected by the emptying of the  $n = 2$  Landau band, as can be seen in the lower panel of Fig. 4. This behavior is accompanied by a rather pronounced splitting of its eigenvalue from the band in the range  $B \approx 4 - 4.5$  T and shown in Fig. 2. The state with eigenfunction  $\Phi_{22}$  is also affected by varying magnetic fields although in a less pronounced fashion, and  $\Phi_{22}$  tends to remain extended throughout the structure except at  $B \approx 8.9$  T, when it is highly peaked around  $j = 25$ .

It is also striking to find in Fig. 1 a sudden global rearrangement of the level structure with respect to  $\mu$ , occurring simultaneously to the total emptying of consecutive Landau bands. This is an unexpected effect produced by the electronic interactions introduced in the self-consistent description of the system, and would not appear in a noninteracting-electron situation. The global rearrangement occurs every time that a Landau band empties. This is propitiated by the varying degeneracy of the magnetic levels, and exhibits smaller “jump” amplitudes for larger Landau band index values (smaller magnetic fields) because of the decreasing fractional charge of each band with respect to the total. This latter feature is evident in Fig. 2 where the level restructuring is less sudden and pronounced. One can also see the global level restructuring in a plot of the total density of states for

various magnetic field values (Fig. 5). This plot, complementary to Fig. 1, shows the total density of states per unit area  $D(E)$ , given by

$$D(E) = (2\pi a_c^2)^{-1} \sum_{m,n,\sigma} g(E - E_{mn\sigma}), \quad (9)$$

where  $g(x)$  is defined by Eq. (7). For fields  $B = 8$  and 10 T, we see the expected symmetric distribution for each Landau band with a total bandwidth  $\approx 4t + 2\Gamma = 4.5$  meV. However, at the emptying of the  $n = 1$  Landau band ( $B \approx 8.9$  T) the function  $D(E)$  is highly asymmetrical and shows a large feature right at the Fermi level which comes mainly from the two SS doublets ( $n = 0$ ,  $\sigma = \pm \frac{1}{2}$ ,  $m = 24, 25$ ).

One very important characteristic of the level structure is the fact that the surfacelike states remain almost stationary in energy across the global level rearrangements, with only a gradual slow drift with respect to  $\mu$  which changes their fractional occupation. This tracking of the Fermi level by the SS levels clearly causes a nonzero density of states at the Fermi level for *all* values of the magnetic field, as is shown in Fig. 6. This “straddling” of the Fermi level by the surfacelike states has a very important consequence: the observed electronic properties of the system in this regime will be strongly influenced by the SS states, and they would be of the utmost importance in a number of experimental configurations such as the quantum Hall effect (see Sec. IV).

As mentioned in the previous section, the boundary conditions imposed on the self-consistent potential  $v(z)$  allow fluctuations of the total amount of negative charge in the superlattice structure. Indeed, while the level structure is undergoing the substantial rearrangement described above, the total electronic charge increases with magnetic field although only slightly. The dimensionless ratio of total negative charge to total positive charge densities,

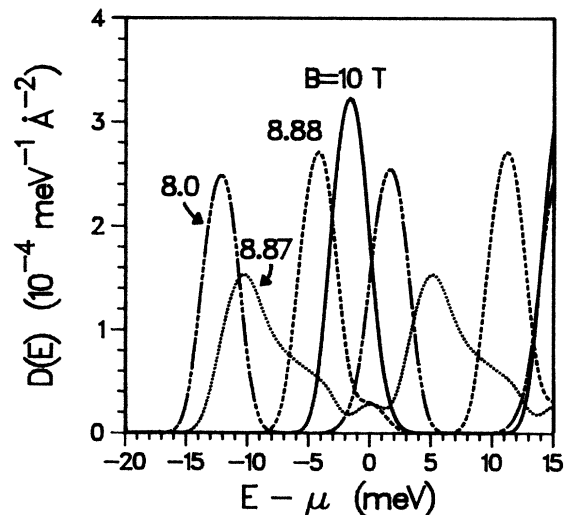


FIG. 5. Total density of states  $D(E)$  of Eq. (9) for several field values near the emptying of the  $n = 1$  Landau band. Structure at the Fermi level for  $B = 8.87$  T is due to SS doublets.

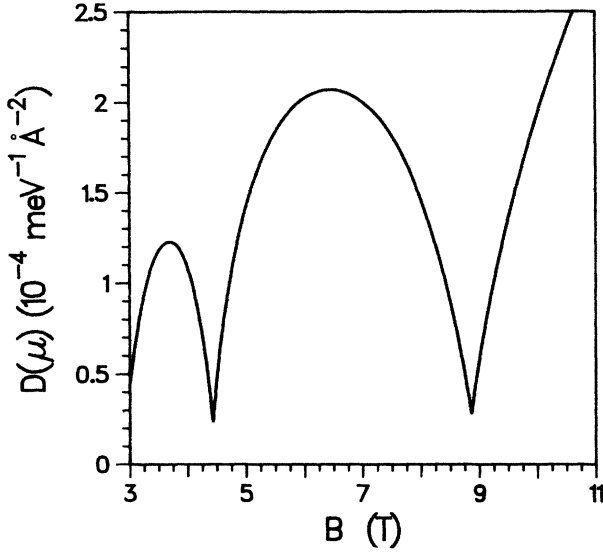


FIG. 6. Density of states at the Fermi level vs magnetic field. Nonzero values at the emptying of the Landau bands ( $B \approx 8.9$  and  $4.5$  T) are due to SS states near  $\mu$ .

$$a\rho_-/\rho_+ = (N\rho_+)^{-1} \sum_j \rho_j, \quad (10)$$

changes from 0.7986 to 0.7992 (or 0.075%) in the range of magnetic field from 3 to 11 T. This small change in the total charge of the system would occur in typical experiments, with the exception of the so-called floating gate arrangements where the total charge in the system can be controlled with great precision.<sup>20</sup> Notice also that the change in the total electronic charge with magnetic field occurs in the semiconducting layers near the ends of the superlattice while the layers in the middle remain with a constant amount of negative charge. This of course is in agreement with the fact that the SS states with varying “filling factors” are peaked mostly near the end layers, and that the associated depletion region extends over only a few layers. Figure 7 shows a typical electronic density profile across the superlattice and the corresponding potential function  $v(z)$ . Notice that the depletion regions at the ends of the superlattice extend over several layers, and are not parabolic, contrary to what the semiclassical treatment in the absence of magnetic field would suggest.

We have also investigated the effect of varying the transparency of the superlattice layers via the hopping parameter  $t$ . In practice, this parameter can be changed over a wide range since it is determined by the alloy concentration and the layer thickness. Figure 8 shows the electronic energy levels of a more “transparent” system which has a larger tunneling parameter than the system of Fig. 1 described so far. In this case we have chosen  $t = 2.5$  meV, four times as large as before,<sup>17</sup> which is reflected in the larger width of the Landau-band quasicontinuum, approximately 10 meV. Some of the main features observed in Fig. 1 also appear here, especially the surfacelike states which track the Fermi level

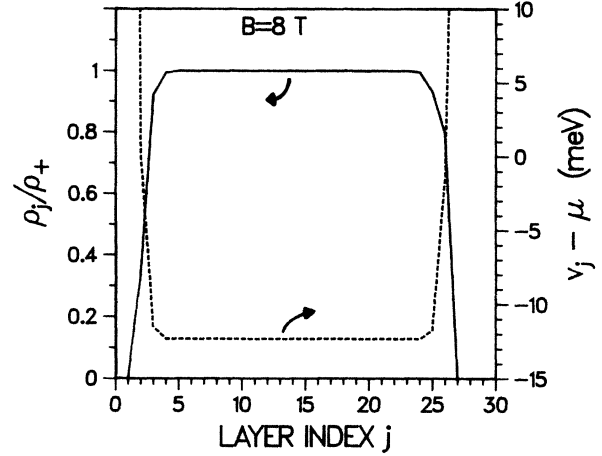


FIG. 7. Electronic density per layer  $\rho_j$  (solid line) and corresponding potential function  $v_j$  for a typical value of magnetic field. Depletion regions on both ends of the structure extend over several layers on each side.

over a range of magnetic fields, and a gradual emptying of the SS states. Notice, however, that the level rearrangement at the emptying of consecutive Landau bands is much less pronounced, and moreover that the precursor QSS states present in Fig. 1 do not appear here. The corresponding QSS eigenvectors, with  $m = 22, 23$ , show no tendency to peak around a layer near the ends of the structure and remain bulklike for all values of field. The larger tunneling parameter has thus smoothed out the sharp level rearrangement seen before, as well as prevented any peel-off precursor of the Landau-band emptying. This is understandable since in the limit of very large  $t$  the system will become completely three dimensional, the

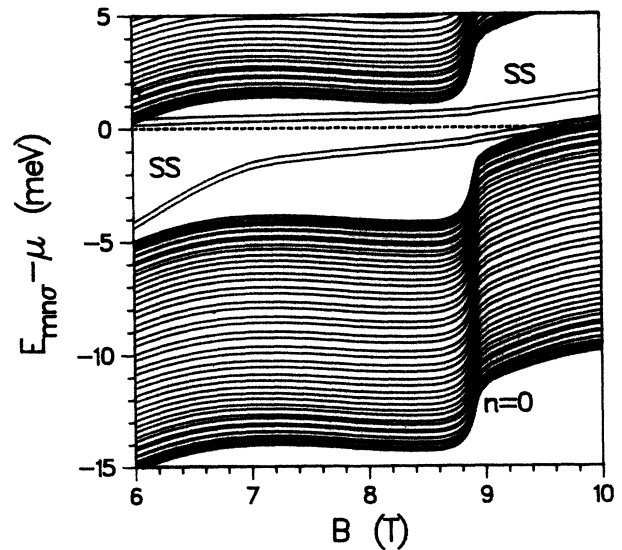


FIG. 8. Level structure for a superlattice with  $t = 2.5$  meV, in the region of  $n = 1$  band emptying. SS doublets are clearly present but QSS are not.

magnetic quantization would not be extreme, and we would have partial occupation of even the bulklike states (since at these values of the field  $\hbar\omega_c$  would be smaller than the z-motion bandwidth).

### B. Effect of gate voltage

As mentioned before, we have also studied the effect of a gate voltage on the electronic level structure of this system. In our calculation we consider the gate voltage to be applied with respect to the middle portion of the structure, where the self-consistent potential function is flat (see Fig. 7). In this scheme, the right-hand side of the superlattice (layer index  $j \approx 30$ ) will have an additional potential bias, while the left-hand side is left untouched.

Figure 9 shows the results of our calculations for a magnetic field value of 8.5 T. The level structure at  $V_G = 0$  corresponds to that shown in Fig. 1 for this  $B$ -field value. It is clear that for increasing bias the total negative charge of the system increases and correspondingly the number of z-motion levels below the Fermi level must increase as well. Figure 9 shows how the levels are pulled below the Fermi level one by one for successively larger voltages. A most important feature of this diagram is the rapid energy shift of the surfacelike states lying in the Landau gap. This sharp variation in energy is of course accompanied by the corresponding change in character of the z-motion eigenfunction  $\Phi_m$ , as verified by direct inspection of the results. This means that the surfacelike states become more and more bulklike as the bias is increased and they eventually join the Landau-band quasicontinuum. This sensitivity of the eigenstates to applied electric fields would allow one to smoothly vary the extension over the rather larger length scale of several superlattice periods. The application of gate volt-

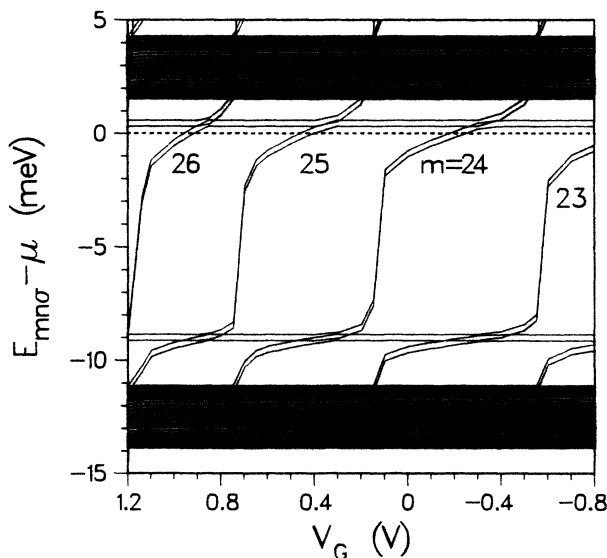


FIG. 9. Level structure of superlattice vs gate voltage  $V_G$  for  $B = 8.5$  T. Only  $n = 0, 1$  Landau bands are shown. All SS levels with an  $m$  label belong to the  $n = 0$  band, and are successively pulled below  $\mu$  for increasing  $V_G$ .

ages would then be a unique probe which drastically changes the physical response of the system, since the SS states are the closest to the Fermi energy and would be most important in a number of experimental situations. Notice also that the rapid energy shift of the SS levels changes their fractional occupation very fast, which would affect the weight of their contribution to physical response functions.

Figure 10 shows the level structure at a larger magnetic field,  $B = 8.87$  T, corresponding to the emptying of the  $n = 1$  Landau band (see Fig. 1). Notice how the SS levels vary rapidly with  $V_G$  in this case as well, despite the fact that the Landau bands are more spread out and the difference between levels in the band and out of it is less pronounced. In fact, the large sensitivity of the SS states to applied gate voltage is present for all values of magnetic field studied.

In Fig. 11 we show the total density of states at the Fermi level for the values of magnetic field of the previous two figures, as a function of the gate voltage. This quantity is of interest since it enters in a number of physical functions such as the magnetoresistance.<sup>13</sup> As one would expect from Figs. 9 and 10,  $D(\mu)$  shows successive maxima as the middle of each SS doublet crosses the Fermi level (recall that  $\Gamma = 1$  meV in this calculation). The crossing of each SS doublet occurs approximately every 0.7 V, although this spacing between levels rapidly decreases for increasing bias by about 0.1-V steps. One can directly compare the bottom trace of this theoretical plot with recent measurements by Störmer *et al.* of the magnetoresistance  $\rho_{xx}$  as a function of the gate voltage.<sup>3(b)</sup> Figure 7 of Ref. 3(b) shows large oscillations in  $\rho_{xx}$  for varying bias with intervals closely in agreement with those of our Fig. 11. However, a detailed comparison of the peaks in  $D(\mu)$  with these experimental results should await calculation of the transport coefficient which takes

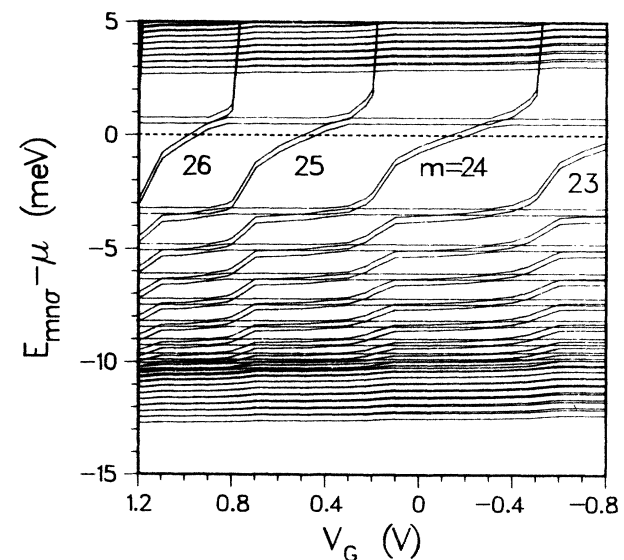


FIG. 10. Level structure vs  $V_G$  for  $B = 8.87$  T. Landau bands are much more spread out at this field value but SS levels still shift rapidly with  $V_G$ .



into consideration the distribution of extended and localized states within the Landau band, as well as the detailed quasiparticle level distribution presented here.

As more and more levels are successively pulled below  $\mu$  for increasing  $V_G$  and their fractional occupation increases, the total negative charge in the system also increases. Figure 12 shows this variation for  $B = 8.5$  T (the corresponding trace for  $B = 8.87$  T is indistinguishable on this scale). We notice linear sections on this curve corresponding to the filling of a particular SS state and joined smoothly by curved segments at voltages which agree with the minima of Fig. 11.

One also notices in Figs. 9 and 10 that while a SS level shifts and its filling changes quickly, the level immediately above it remains only partially filled, close to  $\mu$ , and practically with the same energy. Analysis of the  $z$ -motion eigenfunctions corresponding to the different levels shows that the eigenvector of the nearly flat level is peaked at the left-hand side of the structure (small values of the layer index  $j$ ), in contrast to the SS level which has its eigenvector mostly at large  $j$  values. This is a consequence of the procedure followed in applying the gate voltage, which leaves the left end unchanged with respect to the middle layers of the structure.

#### IV. DISCUSSION

We have presented in the previous sections the results of self-consistent calculations of the electronic level structure of a doped semiconductor superlattice in the Hall configuration for large magnetic fields and simultaneously applied gate voltage.

Let us now discuss the consequences of the calculated level structure for the quantum Hall effect. In the usual two-dimensional systems, at low temperatures and strong magnetic fields, the Hall resistance is quantized to a very

high degree of accuracy according to  $\rho_{xy} = h/\nu e^2$ , where  $\nu$  is an integer, while  $\rho_{xx}$  nearly vanishes.<sup>21</sup> The Hall plateaus are understood in terms of the Fermi level lying in a mobility gap with the integer  $\nu$  being a topological invariant<sup>21,22</sup> related to the number of Landau levels  $r$  having their extended states below the Fermi level. In a single two-dimensional (2D) system  $\nu=r$ , whereas in a multiple-quantum-well stack  $\nu=rs$ , where  $s$  is the number of wells in the stack. The experimentally observed value of  $\nu=48$  reported by Störmer *et al.* for the plateau centered at  $B \approx 8.9$  T is completely consistent with identifying  $\nu$  with the number of broadened levels  $E_{mno}$  whose centers lie below the Fermi energy in our calculation (see Fig. 1, where there are 48 levels below  $\mu$ ). The SS levels have a strong 2D character because of their near confinement to a single GaAs layer, and it is thus reasonable to assume that they would have a very narrow range of extended states at the middle of the broadened  $E_{mno}$  level, in agreement with the results for truly 2D systems.<sup>23</sup> Correspondingly, the activation energy  $\Delta$  of the Hall plateau should be given by the separation between  $\mu$  and the closest surface level extended in the  $x$ - $y$  plane (notice that there are localized states *right at the Fermi level* which come from the tails of the nearby levels as a result of the finite broadening). We find  $\Delta \lesssim 0.5$  meV. This value is over an order of magnitude smaller than the activation energy which one would expect in the absence of surface states (since then one would estimate  $\Delta \approx \hbar\omega_c - W \approx 13$  meV, as explained in Ref. 3). Our calculations thus provide an explanation to the puzzle of the very small activation energy measured by Störmer *et al.*,  $\Delta_{\text{expt}} \approx 0.26$  meV. Precise agreement with experiment can be attained here by small variations of the constants  $\delta$  and  $\delta'$ , or by changing  $\Gamma$ , but this would be somewhat artificial since one expects other effects also to have an impact on this fine tuning.<sup>15</sup> This interpretation also answers the question of why an integer  $\nu$  is observed experimentally even though there is unequal filling of the

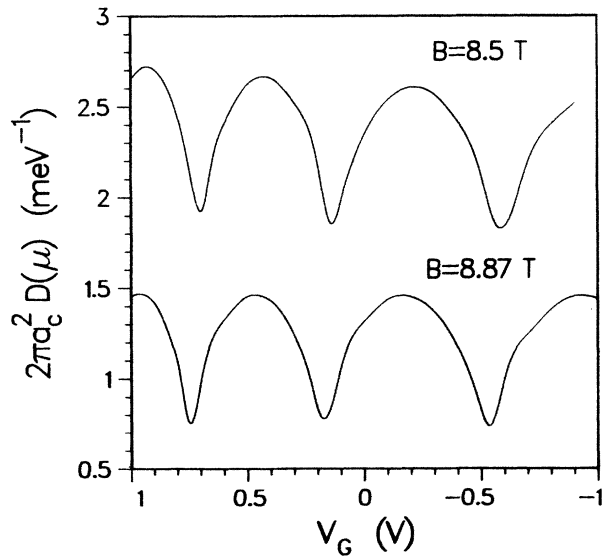


FIG. 11. Density of states at the Fermi level vs gate voltage for two values of magnetic field. Peaks correspond to the middle of SS states successively crossing  $\mu$ .

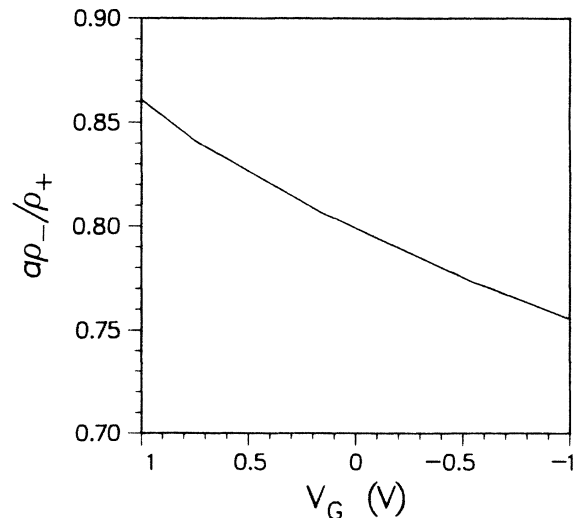


FIG. 12. Total negative charge in the system, Eq. (10), vs gate voltage for  $B = 8.5$  T.



layers in the depletion region and a layer counting argument similar to that of multiple-quantum-well systems would not be valid.

Another consequence of this picture is that by applying a gate voltage one changes the number of levels below  $\mu$ , as seen in Figs. 9 and 10, and this would be expected to change the measured value of  $\nu$ . Störmer *et al.*, anticipating this result with great intuition, have indeed verified that this is the case. They have measured  $\rho_{xy}$  for different gate voltages and found  $\nu$  to vary in steps of two, corresponding to each SS doublet being emptied or filled as the bias varies.<sup>3(b)</sup> It is interesting to notice that the gate voltage would affect the value of  $\Delta$  since it produces shifts of the SS levels. Determination of  $\Delta$  for different gate voltages could provide an alternative and rather direct experimental map of the distribution of extended and localized states within the SS levels.<sup>4-6</sup>

The existence of the surfacelike states should also be important in other experimental situations where the states near the Fermi level are being probed. Examples of this could be the far-infrared resonance of the superlattice, and the collective excitations of the electronic system associated with its surface.<sup>24</sup> Further experimental and theoretical work is needed to assess the impact of these states.

#### ACKNOWLEDGMENTS

We wish to thank H. Störmer and J. Eisenstein for discussions. This work was supported by the Natural Sciences and Engineering Research Council of Canada and by the U.S. Department of Energy, Grant No. DE-FG02-87ER45334.

<sup>1</sup>For recent developments, see *Proceedings of the 18th International Conference on the Physics of Semiconductors, Stockholm, 1986*, edited by O. Engström (World-Scientific, Singapore, 1987).

<sup>2</sup>L. Esaki, *IEEE J. Quantum Electron.* **22**, 1611 (1986).

<sup>3</sup>(a) H. L. Störmer, J. P. Eisenstein, A. C. Gossard, W. Wiegmann, and K. Baldwin, *Phys. Rev. Lett.* **56**, 85 (1986); (b) H. L. Störmer, J. P. Eisenstein, A. C. Gossard, K. W. Baldwin, and J. H. English, in *Proceedings of the 18th International Conference on the Physics of Semiconductors, Stockholm, 1986*, Ref. 1, p. 385.

<sup>4</sup>J. P. Eisenstein, H. L. Störmer, V. Narayanamurti, A. Y. Cho, A. C. Gossard, and C. W. Tu, *Phys. Rev. Lett.* **55**, 875 (1985).

<sup>5</sup>M. Ya. Azbel, *Phys. Rev. B* **33**, 8844 (1986).

<sup>6</sup>P. A. Lee and T. V. Ramakrishnan, *Rev. Mod. Phys.* **57**, 287 (1985).

<sup>7</sup>R. Dingle, H. L. Störmer, A. C. Gossard, and W. Wiegmann, *Appl. Phys. Lett.* **33**, 665 (1978).

<sup>8</sup>T. Haavasoja, H. L. Störmer, D. J. Bishop, V. Narayanamurti, A. C. Gossard, and W. Wiegmann, *Surf. Sci.* **142**, 294 (1984).

<sup>9</sup>R. C. Miller, W. T. Tsang, and O. Munteanu, *Appl. Phys. Lett.* **41**, 374 (1982); M. H. Meynadier, J. A. Brum, C. Delalande, M. Voos, F. Alexandre, and J. L. Lievin, *J. Appl. Phys.* **58**, 4307 (1985).

<sup>10</sup>A preliminary report of some of these results has appeared, S. E. Ulloa and G. Kirczenow, *Phys. Rev. Lett.* **57**, 2991 (1986).

<sup>11</sup>R. C. Miller, D. A. Kleinman, and A. C. Gossard, *Phys. Rev. B* **29**, 7085 (1984), and references therein.

<sup>12</sup>Higher Kronig-Penney minibands are not expected to have a large effect in the description of electronic states if the self-consistent potential  $v(z)$  appearing in Eq. (1) varies slowly with position.

<sup>13</sup>See for example, J. M. Ziman, *Principles of the Theory of Solids*, 2nd ed. (Cambridge University, Cambridge, England, 1972).

<sup>14</sup>See for example, L. D. Landau and E. M. Lifshitz, *Quantum*

*Mechanics*, 3rd ed. (Pergamon, Oxford, 1977), Chap. XV.

<sup>15</sup>The bare value in GaAs,  $g=0.52$ , is used in this calculation. Exchange enhancement effects [Th. Englert, D. C. Tsui, A. C. Gossard, and Ch. Uihlein, *Surf. Sci.* **113**, 295 (1982)] are ignored in this choice, in agreement with the experiment of Ref. 3 which did not find evidence for  $g$  enhancement in this system.

<sup>16</sup>T. Ando, A. B. Fowler, and F. Stern, *Rev. Mod. Phys.* **54**, 437 (1982); S. Das Sarma and F. Stern, *Phys. Rev. B* **32**, 8442 (1985).

<sup>17</sup>The values of the various parameters used in the calculations of Sec. III are as follows:  $m=0.067m_e$ ,  $\epsilon=12.5$ ,  $a=226 \text{ \AA}$ ,  $L=1100 \text{ \AA}$ ,  $t=0.625 \text{ meV}$ ,  $\rho_+/a=1.9 \times 10^{17} \text{ cm}^{-3}$ ,  $\delta=1.6 \text{ eV}$ ,  $\delta'=1.3 \text{ eV}$ , and  $\Gamma=1 \text{ meV}$ . Notice that we neglect differences in the electronic effective mass between GaAs and  $\text{Al}_x\text{Ga}_{1-x}\text{As}$ , and  $\epsilon$  is taken as the average value of the dielectric constant in the two constituent semiconducting layers. The constant value of the Fermi energy  $\mu$  is assumed to be determined by the physical connections between the system and the exterior. This describes the typical experimental situation in which the total charge in the system is not kept constant (however, see Ref. 20).

<sup>18</sup>H. L. Störmer, A. C. Gossard, and W. Wiegmann, *Appl. Phys. Lett.* **39**, 493 (1981).

<sup>19</sup>For a review on gated heterostructures, see H. Sakaki, *IEEE J. Quantum Electron.* **22**, 1845 (1986).

<sup>20</sup>R. T. Zeller, F. F. Fang, B. B. Goldberg, S. L. Wright, and P. J. Stiles, *Phys. Rev. B* **33**, 1529 (1986).

<sup>21</sup>*The Quantum Hall Effect*, edited by R. E. Prange and S. E. Girvin (Springer-Verlag, New York, 1987).

<sup>22</sup>R. B. Laughlin, *Phys. Rev. B* **23**, 5623 (1982); Q. Niu, D. J. Thouless, and Y. S. Wu, *ibid.* **31**, 3372 (1985).

<sup>23</sup>H. Aoki and T. Ando, *Phys. Rev. Lett.* **54**, 831 (1985), and references therein.

<sup>24</sup>J. K. Jain and S. Das Sarma, *Phys. Rev. B* **35**, 918 (1987).

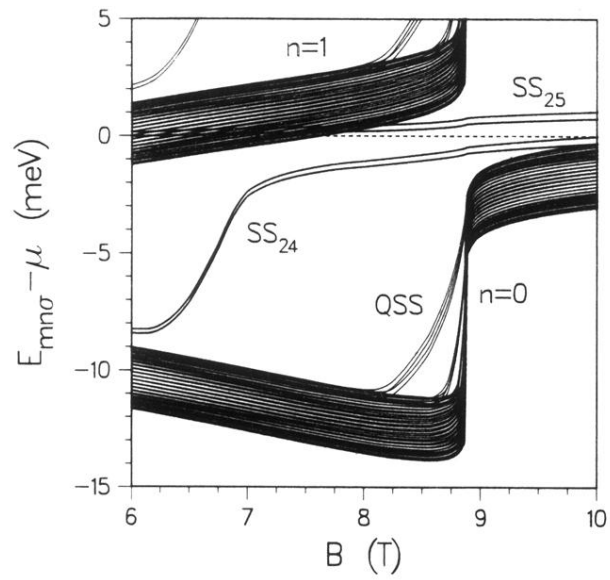


FIG. 1. Energy levels  $E_{mn\sigma}$  of a tunneling superlattice with respect to the Fermi energy  $\mu$  (dashed line) for lowest Landau indices  $n$ . Only center of each broadened level is shown ( $\Gamma=1$  meV).  $SS_m$  spin doublets correspond to the quantum numbers  $\sigma = \pm\frac{1}{2}$ ,  $n=0$ , and  $m=24$  (25) for levels below (above)  $\mu$ . QSS doublets correspond to  $\sigma = \pm\frac{1}{2}$ ,  $n=0$ , and  $m=22,23$ .

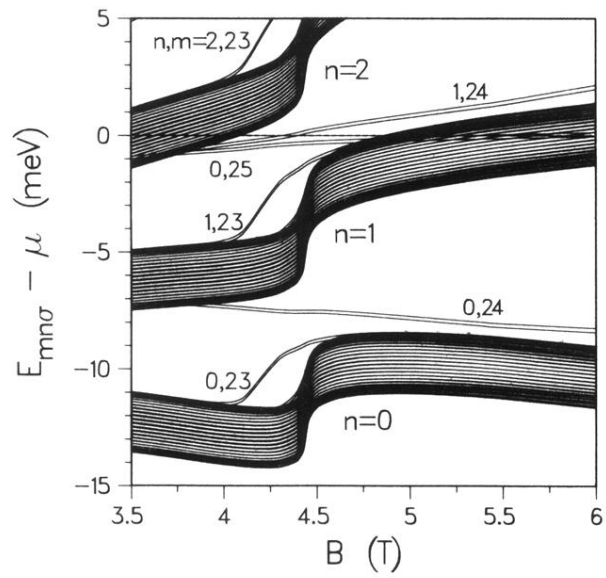


FIG. 2. Level structure at lower magnetic field. Here, the  $n = 2$  band is being emptied. Notice SS states also present in the Landau gap regions. These spin doublets ( $\sigma = \pm \frac{1}{2}$ ) are labeled by their quantum numbers  $n, m$ .

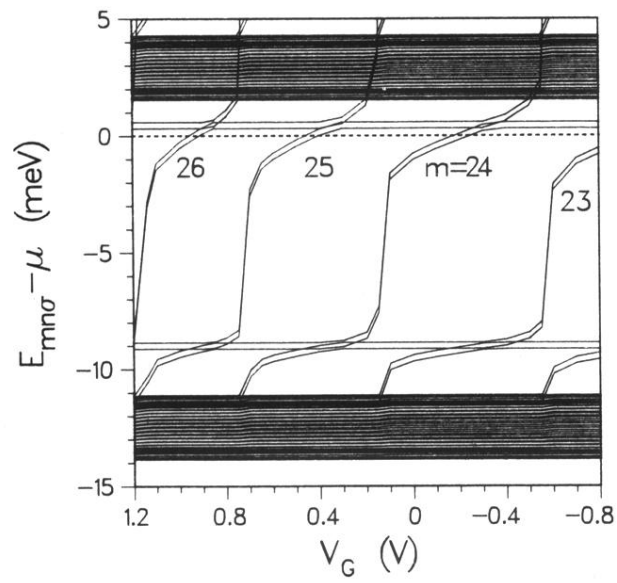


FIG. 9. Level structure of superlattice vs gate voltage  $V_G$  for  $B = 8.5$  T. Only  $n = 0, 1$  Landau bands are shown. All SS levels with an  $m$  label belong to the  $n = 0$  band, and are successively pulled below  $\mu$  for increasing  $V_G$ .